

# CoD: A Diffusion Foundation Model for Image Compression

Zhaoyang Jia<sup>1\*</sup> Zihan Zheng<sup>1\*</sup> Naifu Xue<sup>2\*</sup> Jiahao Li<sup>3</sup> Bin Li<sup>3</sup>  
Zongyu Guo<sup>3</sup> Xiaoyi Zhang<sup>3</sup> Houqiang Li<sup>1</sup> Yan Lu<sup>3</sup>

<sup>1</sup> University of Science and Technology of China <sup>2</sup> Communication University of China  
<sup>3</sup> Microsoft Research Asia

{jzy\_ustc, zzh2003}@mail.ustc.edu.cn, lihq@ustc.edu.cn, {aaronxuef}@cuc.edu.cn  
{libin, li.jiahao, zongyuguo, xiaoyizhang, yanlu}@microsoft.com

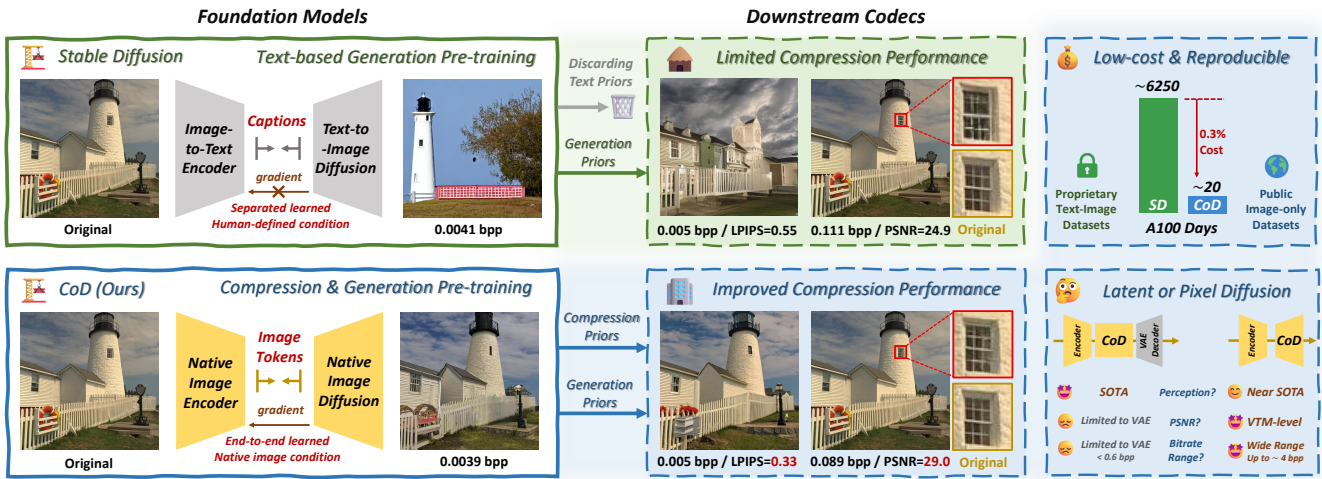


Figure 1. Overview of Compression-oriented Diffusion (CoD) foundation models, which are trained from scratch to jointly optimize compression and generation. Rather than a fixed codec, CoD serves as a foundational model for downstream diffusion-based codecs such as DiffC [43], substantially enhancing their performance by replacing Stable Diffusion.

## Abstract

Existing diffusion codecs typically build on text-to-image diffusion foundation models like Stable Diffusion. However, text conditioning is suboptimal from a compression perspective, hindering the potential of downstream diffusion codecs, particularly at ultra-low bitrates. To address it, we introduce **CoD**, the first **Compression-oriented Diffusion** foundation model, trained from scratch to enable end-to-end optimization of both compression and generation. CoD is not a fixed codec but a general foundation model designed for various diffusion-based codecs. It offers several advantages: **High compression efficiency**, replacing Stable Diffusion with CoD in downstream codecs like DiffC achieves SOTA results, especially at ultra-low bitrates (e.g., 0.0039 bpp); **Low-cost and reproducible training**, 300× faster training than Stable Diffusion (~20 vs. ~6,250 A100 GPU days) on

entirely open image-only datasets; **Providing new insights**, e.g., We find pixel-space diffusion can achieve VTM-level PSNR with high perceptual quality and can outperform GAN-based codecs using fewer parameters. We hope CoD lays the foundation for future diffusion codec research. Codes are released at <https://github.com/microsoft/GenCodec/tree/main/CoD>.

## 1. Introduction

Diffusion image compression [7, 15, 27, 32, 37, 46, 54] exploits the strong generative priors of denoising diffusion models [21, 33, 42] to achieve realistic image reconstruction. To inherit such generative priors, recent diffusion codecs typically adopt large-scale pretrained text-to-image diffusion models such as Stable Diffusion [39], demonstrating impressive performance in generative image compression.

However, when using text-to-image diffusion models in

\*This work was done when Zhaoyang Jia, Zihan Zheng and Naifu Xue were full-time interns at Microsoft Research Asia.

compression, the role of text conditions remains unclear. Although early works such as Text+Sketch [29] and PerCo [7] claim image captions can serve as a high-level semantic signal to facilitate ultra-low bitrate compression, later studies [15, 53] demonstrate that fine-tuning Stable Diffusion to discard text priors can further improve compression efficiency. Additional evidence comes from the zero-shot diffusion compression framework DiffC [46], which theoretically measures the “compression capability” of a denoising diffusion model. When applied to Stable Diffusion, DiffC reveals that text conditions are detrimental to compression performance, especially at low bitrates. These observations suggest that text-conditioned diffusion models are not naturally suitable for compression, and that **Stable Diffusion is not the ideal foundation model for diffusion codecs**.

To understand this phenomenon, we analyze the underlying mechanism. In a standard compression formulation,

$$y = \text{Encode}(x, \Theta), \quad \hat{x} = \text{Decode}(y, \Phi) \quad (1)$$

where  $x$ ,  $y$ , and  $\hat{x}$  denote the original image, compressed representation, and reconstruction, respectively, and  $\Theta$  and  $\Phi$  represent the trained parameters of the encoder and decoder. If we set  $\Theta$  as an image captioner like BLIP-2 [30] and  $\Phi$  as Stable Diffusion, we note that *text-conditioned diffusion can be formulated in the compression formulation*, as illustrated in the top left of Figure 1. From the perspective of compression, text conditions introduces two limitations. First, human-generated text is less efficient in describing fine-grained spatial and texture details of natural images. Second, the discrete vocabularies in text is non-differentiable to prevent joint optimization of  $\Theta$  and  $\Phi$ , thus making rate–distortion optimization inapplicable.

Recognizing the limitations of text conditions, a natural next step is to **train a diffusion foundation model explicitly oriented toward compression**. Neural codecs can learn compact, native image tokens as conditions for diffusion models, and enable end-to-end training with the diffusion model to determine the optimal image representations for coding. By carefully designing and leveraging advanced diffusion training algorithms, we introduce the first **Compression-oriented Diffusion foundation model, CoD**. The architecture of CoD is simple yet effective: a native image encoder  $\Theta$  to compress images into tokens, followed by an information bottleneck, and a diffusion model  $\Phi$  to decode pixels conditioned on these image tokens. The bottleneck is designed to enforce ultra-low bitrates (e.g., 0.0039 bpp), transmitting only essential semantic information while allowing the diffusion model the flexibility to generate realistic details. As illustrated in the bottom left of Figure 1, CoD achieves significantly higher reconstruction fidelity compared to text-to-image foundation models.

It is worth noting that CoD is not a fixed codec but a general foundation model designed for diverse diffusion-

based compression algorithms. In practice, it can replace Stable Diffusion in existing downstream diffusion codecs to improve performance. Unlike Stable Diffusion that only provides generation priors, CoD additionally learns compression priors to substantially boost downstream performance, particularly at low bitrates. CoD offers several advantages:

**Low Training Cost.** Compared to Stable Diffusion, CoD is far more efficient to train. Stable Diffusion v1.5 requires about 6,250 A100 GPU days [8], whereas CoD only takes around 20 A100 GPU days (0.3% cost). Unlike text-to-image diffusion that relies on text-image training pairs, CoD is fully self-supervised and only requires image datasets, making it easier to scale. Furthermore, while Stable Diffusion uses proprietary datasets, CoD is trained entirely on open datasets such as ImageNet [40], OpenImages [26], and SA-1B [25], making it easy to reproduce and unleashing the potential for future exploration across different diffusion codec architectures and training schemes.

**Providing New Insights.** We conduct an in-depth analysis of CoD to gain insights into diffusion-based compression. We facilitate scaling-law study of CoD to reveal how model size affects compression performance. We further show that diffusion codecs can surpass GAN-based codecs even with significantly fewer parameters. In addition, we present a comprehensive comparison between pixel-space and latent-space diffusion. While latent diffusion offers superior perceptual quality at low bitrates, its PSNR and bitrate range are constrained by the VAE (e.g., up to  $\sim 26$  dB PSNR at 0.6 bpp). In contrast, pixel diffusion delivers both high perceptual quality and high PSNR across a wide bitrate range (e.g., reaching near-lossless  $\sim 47$  dB PSNR at 4 bpp).

**High Compression Performance.** As a compression-oriented foundation model, CoD enables high-performance downstream codecs. In this paper, we evaluate it using the state-of-the-art zero-shot diffusion compression method, DiffC [43, 46]. Compared to Stable Diffusion, DiffC with CoD achieves significantly better performance, especially at low bitrates. With pixel-space CoD, it even matches VTM [47] in PSNR while outperforming previous pixel-space perceptual codecs such as MS-ILLM [36] in FID. The qualitative results in middle column of Figure 1 demonstrate that pixel-space CoD achieves much higher reconstruction fidelity, highlighting the potential of pixel diffusion to approach the theoretical rate–distortion–perception trade-off.

The contributions of this work can be summarized as:

- We introduce the first compression-oriented diffusion foundation model, CoD, designed to replace Stable Diffusion in diffusion codecs.
- CoD enables low-cost, reproducible training, supporting exploration of new network architectures.
- CoD delivers high compression performance, especially on ultra-low bitrates.
- CoD pushes the boundaries of diffusion codecs, demon-

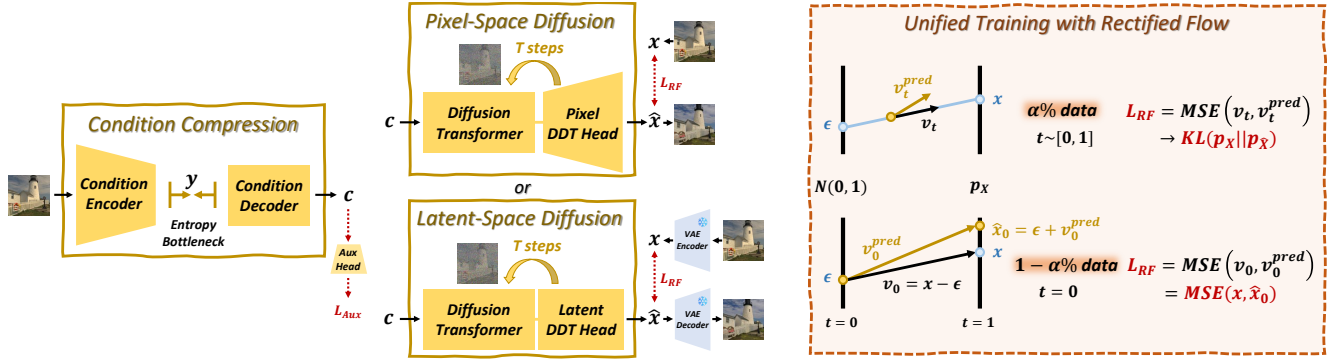


Figure 2. Framework overview of CoD in pixel and latent spaces. CoD consists of a condition encoder, an entropy bottleneck, a condition decoder and a diffusion model which is decoupled to DiT backbone and DDT head [49]. CoD is trained with rectified flow [33], where  $1 - \alpha\%$  samples are trained at  $t = 0$  to jointly optimize distortion and perception.

strating the potential of pixel-space diffusion as a pathway toward the optimal rate–distortion–perception trade-off.

## 2. Compression-oriented Diffusion

In this section, we introduce the implementation details of the proposed compression-oriented diffusion models, CoD.

### 2.1. Pipeline

We implement CoD in both pixel and latent spaces. As illustrated in Figure 2, given an input data  $x$ , CoD performs: **Condition Encoding**. An encoder firstly compresses  $x$  into compact representations. Following [12], we stack residual blocks [18] and attention layers [45] to construct the encoder. The output is at  $1/32$  resolution of the original images.

**Entropy bottleneck**. It is designed to maintain an ultra-low bitrate for  $y$ , encouraging the diffusion model to learn strong generative capabilities. This can be implemented as scalar quantization with entropy models [5], vector quantization [12], or finite scalar quantization [35]. For simplicity, we use vector quantization with a codebook size of  $N = 2^4 = 16$ , corresponding to 4 bits/ $(32 \times 32) = 0.0039$  bpp.

**Condition Decoding**. The condition decoder reconstructs intermediate compression conditions  $c$  from the image tokens  $y$ . The decoder adopts similar structures as the encoder. The condition  $c$  is at a  $1/16$  resolution of the original image. **Diffusion-based reconstruction**. The diffusion module denoises a randomly sampled Gaussian noise over  $T$  steps under the guidance of condition  $c$  to reconstruct  $\hat{x}$ . Following DDT [49], we decouple DiT backbone and DDT head to enhance capacity. DDT performs denoising at  $1/16$  resolution, where the condition  $c$  is concatenated with the noised input along the channel dimension at each step for guidance.

In the latent space, since VAE latents are already at  $1/8$  resolution, we apply a  $2 \times 2$  patch embedding to downsample them to  $1/16$ , and upsample the output of DDT head back to  $1/8$  before passing to the VAE decoder. In the pixel space,

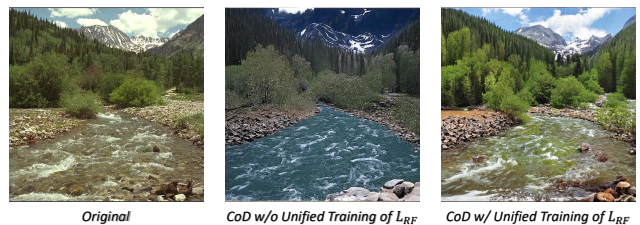


Figure 3. Effects of unified training with rectified flow.

we directly use a  $16 \times 16$  patch embedding to map the noised images to  $1/16$  resolution, and adopt the pixel DDT head from [48], where each feature predicts a neural field that reconstructs a corresponding  $16 \times 16$  patch. Since the DiT backbone runs at  $1/16$  resolution of original images, **pixel-space CoD has a similar computation complexity as in latent space**. Details are in the appendix.

### 2.2. Diffusion Training

**Preliminary**. Denoising diffusion models [46] model the data distribution by progressively perturbing a clean sample  $x$  with Gaussian noise  $\varepsilon$ , transforming  $p(x)$  into a standard Gaussian distribution. At timestep  $t$ , it is formulated as,

$$x_t = \alpha_t x + \sigma_t \varepsilon, \quad \varepsilon \sim \mathcal{N}(0, I) \quad (2)$$

where  $\alpha_t$  and  $\sigma_t$  define the noise schedule. The process can be expressed as a stochastic differential equation (SDE),

$$dx_t = f(t) x_t dt + g(t) d\omega_t \quad (3)$$

with drift  $f(t)$  and diffusion  $g(t)$  determined by  $\alpha_t$  and  $\sigma_t$ . Score-based models [42] learn the score function of  $p(x)$  to solve the reverse SDE and generate samples.

Rectified Flow (RF) [33] reinterprets diffusion as a deterministic transformation. It removes the stochastic term from the SDE and adopts a linear transition schedule:

$$x_t = t \cdot x + (1 - t) \cdot \varepsilon. \quad (4)$$

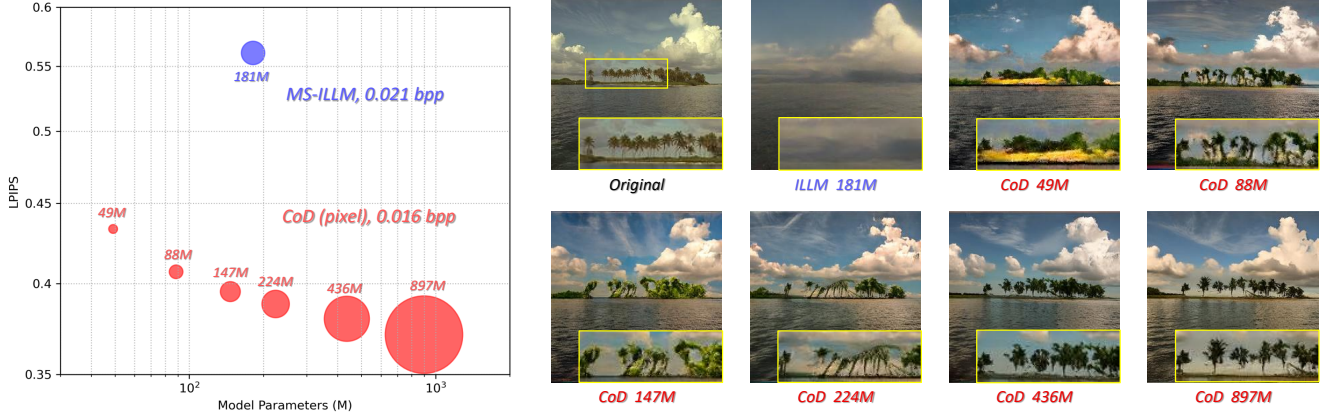


Figure 4. Scaling law analysis on Kodak at  $256 \times 256$ . All CoD models are at 0.016 bpp while MS-ILLM is at 0.021 bpp.

So the trajectory follows a simple ordinary differential equation (ODE) formulated as:

$$dx_t = v_t dt, \quad \text{where } v_t = x - \varepsilon \quad (5)$$

Instead of estimating the score, RF directly learns the velocity field  $v_t$ , providing more stable training, faster inference, and a clearer geometric view of generation.

**Unified Training with Rectified Flow.** CoD predicts the velocity  $v_t$  so it can be trained with the rectified flow loss,

$$\mathcal{L}_{\text{RF}} = \text{MSE}(v_t, v_t^{\text{pred}}) \quad (6)$$

where  $v_t^{\text{pred}}$  denotes the predicted velocity field. Theoretically, optimizing  $\mathcal{L}_{\text{RF}}$  reduces the Kullback–Leibler (KL) divergence between the reconstructed and original distributions [13], which can reflect the perception term in rate-distortion-perception (R-D-P) theory [6]. Hence, optimizing  $\mathcal{L}_{\text{RF}}$  naturally promotes perceptual quality.

However, we find that rectified flow loss mainly guarantee the reconstruction consistency of the structure instead of color information (see Figure 3). From a compression viewpoint, this is consistent with R–D–P theory: standard diffusion training neglects the distortion term, leading to limited reconstruction fidelity.

To overcome this, we introduce a unified formulation that integrates a distortion term into the rectified flow loss. Since the one-step estimate at  $t = 0$  is  $\hat{x}_0 = \varepsilon + v_0^{\text{pred}}$ , the rectified flow loss can be rewritten given  $v_0 = x - \varepsilon$ :

$$\mathcal{L}_{\text{RF}} = \text{MSE}(v_0, v_0^{\text{pred}}) = \text{MSE}(x, \hat{x}_0) \quad (7)$$

Thus, optimizing  $\mathcal{L}_{\text{RF}}$  at  $t = 0$  directly minimizes one-step reconstruction distortion to incorporate a distortion term during training. As illustrated in Figure 2, during training we randomly select  $\alpha\%$  samples with  $t \in [0, 1]$  and the rest with  $t = 0$  to enable the unified training.

**Discussion.** Unified training is designed for continuous flows, where the probability of sampling a fully noised state

$t = 0$  approaches zero. We observe that color reconstruction in CoD is largely determined by its first denoising step; thus, the absence of  $t = 0$  optimization often leads to noticeable color shifts. In contrast, DDPM-based codecs such as PerCo [7] employ discrete timesteps uniformly sampled as  $t_{\text{DDPM}} \in 1, \dots, 1000$ , inherently including optimizing of fully noised state. This can be viewed as a special case of our formulation with  $1 - \alpha\% = 1/1000$ .

### 2.3. Implementation Details

**Datasets.** Foundation models require large-scale training to achieve optimal performance. Unlike text-to-image generation that depends on text-image data pairs, CoD is fully self-supervised and requires only image datasets, making large-scale scaling more accessible. In this paper, we use ImageNet-21K [40], OpenImage [26] and SA-1B [25], including a total of 22M images. All datasets are publicly available, facilitating reproducibility for future research.

**Loss Function.** For the information bottleneck, we adopt the codebook commitment loss  $\mathcal{L}_C$  [12]. Diffusion training employs the rectified flow loss  $\mathcal{L}_{\text{RF}}$  and the representation alignment loss  $\mathcal{L}_{\text{REPA}}$  with DINOv2 [38]. Additionally, an auxiliary head (Figure 2) reconstructs both original pixels and DINOv2 features from the condition  $c$  to enhance condition learning. Further analysis of this auxiliary loss  $\mathcal{L}_{\text{aux}}$  is in the appendix. The overall objective is

$$\mathcal{L} = \mathcal{L}_{\text{RF}} + \lambda \cdot \mathcal{L}_{\text{REPA}} + \beta \cdot \mathcal{L}_C + \gamma \cdot \mathcal{L}_{\text{aux}} \quad (8)$$

where  $\lambda = 0.5$ ,  $\beta = 0.25$  and  $\gamma = 1.0$ .

**Training Details.** We incorporate several advanced techniques for diffusion training. Timesteps are sampled following a log-normal distribution, which is further enhanced by the unified training strategy introduced in Section 2.2. CoD is progressively trained from low to high resolution: first at  $256 \times 256$  for 400k steps with a batch size of 128, and then fine-tuned at  $512 \times 512$  for 150k steps with a batch size of 64. The encoder downsamples images to  $1/16$  at  $256 \times 256$

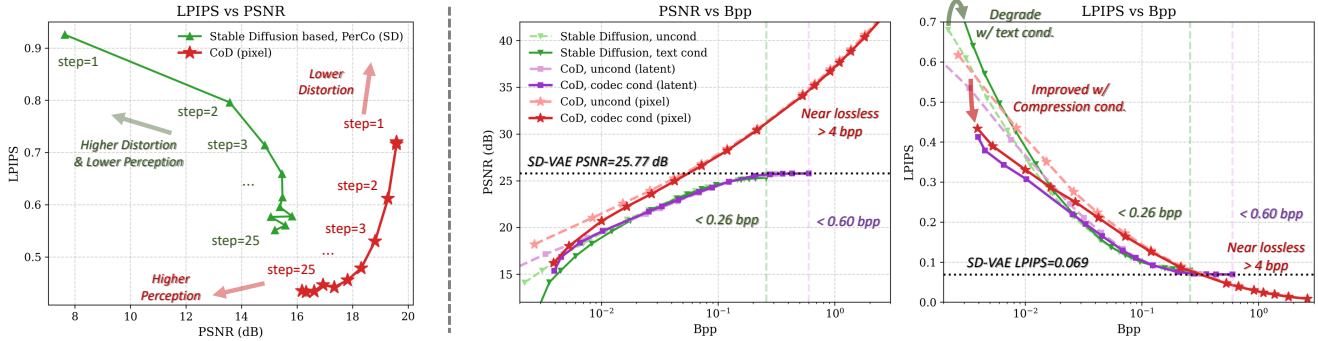


Figure 5. Comparison of CoD and Stable Diffusion on Kodak at  $512 \times 512$  resolution. (left) Pixel-space CoD enables zero-shot distortion-perception controlling by adjusting the sampling steps. CoD is at 0.0039 bpp and PerCo is at 0.0036 bpp. (right) Text conditions harms performance of zero-shot algorithm DiffC on Stable Diffusion, while CoD condition boosts LPIPS at low-bitrate. In addition, pixel-space CoD is not limited by the SD-VAE thus demonstrating wider bitrates, higher PSNR and higher potential in perceptual quality.

resolution (0.0156 bpp) and to  $1/32$  at  $512 \times 512$  (0.0039 bpp), ensuring that the total number of patches and overall bit cost remain consistent.

**Training Costs.** CoD is trained on 4 NVIDIA A100 GPUs for approximately 5 days, totaling around 20 A100 GPU days. This represents only about 0.3% of the training cost of Stable Diffusion v1.5 [39], primarily because: (1) CoD learns the most informative compression conditions end-to-end, rather than relying on high-dimensional, human-defined text embeddings; (2) the unified rectified flow training stabilizes and accelerates convergence; (3) advanced optimization strategies such as REPA [56] further improve efficiency.

**Diffusion Sampling.** For ODE-based sampling, we employ the Adam-like-2nd solver [48] with 25 steps. We use classifier-free guidance [20] with scales of 3.0 for pixel space and 1.25 for latent space to enhance conditional generation.

### 3. Analysis on Foundation Model

In this section, we conduct an in-depth analysis of CoD to investigate its performance and underlying characteristics. More analysis are in the appendix.

#### 3.1. Evaluation

CoD naturally operates as a codec at 0.0039 bpp. We evaluate its compression performance on the Kodak [10] dataset at  $512 \times 512$  resolution. To ensure fair comparison among foundation models, we employ the same SD-VAE and compare our latent-space CoD with Stable-Diffusion-based codecs, including zero-shot DiffC [46], DDCM [37], and fine-tuned PerCo (SD) [27] and OSCAR [15]. As shown in Figure 6, CoD achieves superior reconstruction quality. A more detailed quantitative comparison is presented in Section 4.

#### 3.2. Scaling Law

Most diffusion codecs are constrained by the parameter count of Stable Diffusion (approximately 860M), making it dif-



Figure 6. Visual comparison between Stable-Diffusion-based codecs and latent-space CoD under ultra-low bitrates.

ficult to study parameter scaling. It also remains unclear whether the performance advantages of diffusion codecs over GAN-based codecs (e.g., MS-ILLM [36]) stem from architectural improvements or simply from model scaling. To explore this, we train pixel-space CoDs with varying channel dimensions at  $256 \times 256$  resolution for 400k steps and evaluate them on Kodak. As shown in Figure 4, we observe a clear trend: increasing model parameters consistently enhances compression performance. Compared with the GAN-based MS-ILLM (181M parameters), CoD achieves notably better reconstruction quality even with only 49M parameters, confirming that the performance gain primarily originates from algorithmic improvements rather than model size.

#### 3.3. Zero-Shot Distortion-Perception Control

The proposed unified training jointly optimizes one-step distortion and multi-step perception, endowing CoD with the ability to control the distortion-perception trade-off directly through the number of sampling steps. As shown in Fig-

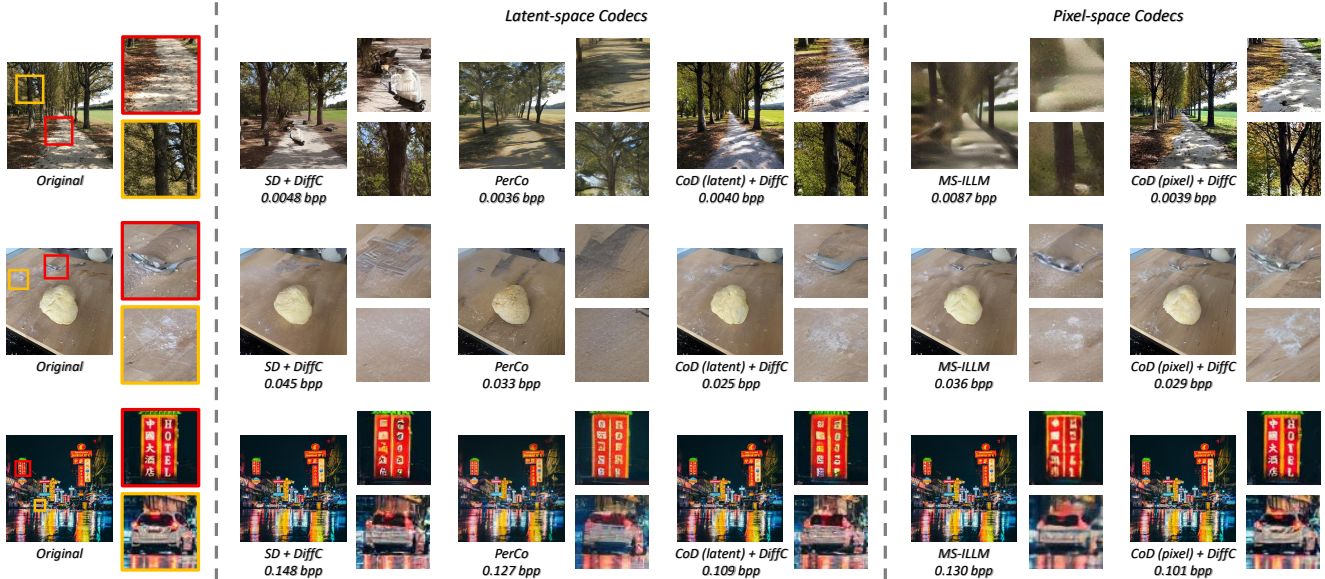


Figure 7. Visualization comparison on the CLIC2020 test set across bitrates from low (top) to high (bottom).

ure 5 (left), at 0.0039 bpp, pixel-space CoD attains the best perceptual quality at 25 steps and achieves a 3.4 dB PSNR improvement (from 16.2 dB to 19.6 dB) when reduced to a single step. Intermediate step counts smoothly interpolate between these two states. In contrast, diffusion codecs without this formulation (e.g., PerCo (SD)) fail to exhibit such controllable improvement through step reduction.

### 3.4. Revisiting Pixel-Space Diffusion

Recent diffusion codecs typically operate in the latent space of a KL-VAE, achieving impressive results at low bitrates (e.g.,  $<0.1$  bpp). However, their performance is fundamentally constrained by the entropy and reconstruction capacity of the underlying VAE. As shown in Figure 5 (right), DiffC [46] built on Stable Diffusion cannot surpass the reconstruction limit of the SD-VAE (PSNR 25.77 dB, LPIPS 0.069), with a bitrate ceiling around 0.26 bpp. Similarly, latent-space CoD remains bounded by VAE quality even up to 0.60 bpp, indicating that latent diffusion codecs inherently operate within a limited quality and bitrate range.

In contrast, pixel-space CoD directly models raw pixels to overcome this constraint. It can scale the bitrate beyond 1.0 bpp while continuously improving reconstruction quality. Pixel-space CoD surpasses latent diffusion models in LPIPS at around 0.3 bpp and maintains substantially higher PSNR across the entire range. This demonstrates the potential of pixel-space diffusion as a more general and unconstrained approach to learned compression in future research.

## 4. Downstream Compression Performance

In this section, we conduct a comprehensive evaluation of CoD when integrated into downstream compression frame-

works. Since most diffusion-based codecs do not release their training code, we employ the zero-shot compression method DiffC [46] on CoD for comparison. **Additional downstream results are presented in the appendix, e.g., fine-tuning one-step CoD achieves real-time and SOTA performance (Section B), and CoD-based perceptual loss that significantly enhances MS-ILLM [36] performance (Section C).** **Benchmarks and Baselines.** Experiments are conducted on the Kodak [10], CLIC2020 test set [44] and Div2K [1]. All images are resized and center-cropped to a resolution of  $512 \times 512$ . We report distortion using PSNR and perceptual quality using LPIPS [57], DISTs [9], and FID [19]. Following [37], FID is computed on extracted patches ( $64 \times 64$  for Kodak and  $128 \times 128$  for CLIC2020). Bitrate is measured in bits per pixel (bpp). In addition to diffusion codecs (DiffC, DDCM, PerCo (SD), and OSCAR; see Section 3.1), we further compare against the latent-space codec DiffeIC [32] and pixel-space codecs including the traditional codec VTM [47] and perceptual codecs HiFiC [34], MS-ILLM [36], CDC [54] and TACO [28]. We also discuss StableCodec [58] and OneDC [53] which are built on pretrained one-step diffusion models in the appendix.

**Pixel-space Comparison.** The rate-distortion curves on pixel space codecs are shown in Figure 8. Pixel space codecs are free of the limitation of VAE latents thus can achieve wider bitrates and quality ranges. Across all bitrates, our codec achieves superior PSNR, DISTs and FID values. Notably, perceptual codecs HiFiC, MS-ILLM, CDC ( $\rho = 0.9$ ) and TACO are optimized with LPIPS, whereas pixel-space CoD is not, which explains performance on LPIPS.

Surprisingly, our codec achieves comparable BPP-PSNR performance to VTM (BD-Rate is  $-2.1\%$  using VTM as anchor) while delivering significantly better perceptual quality.

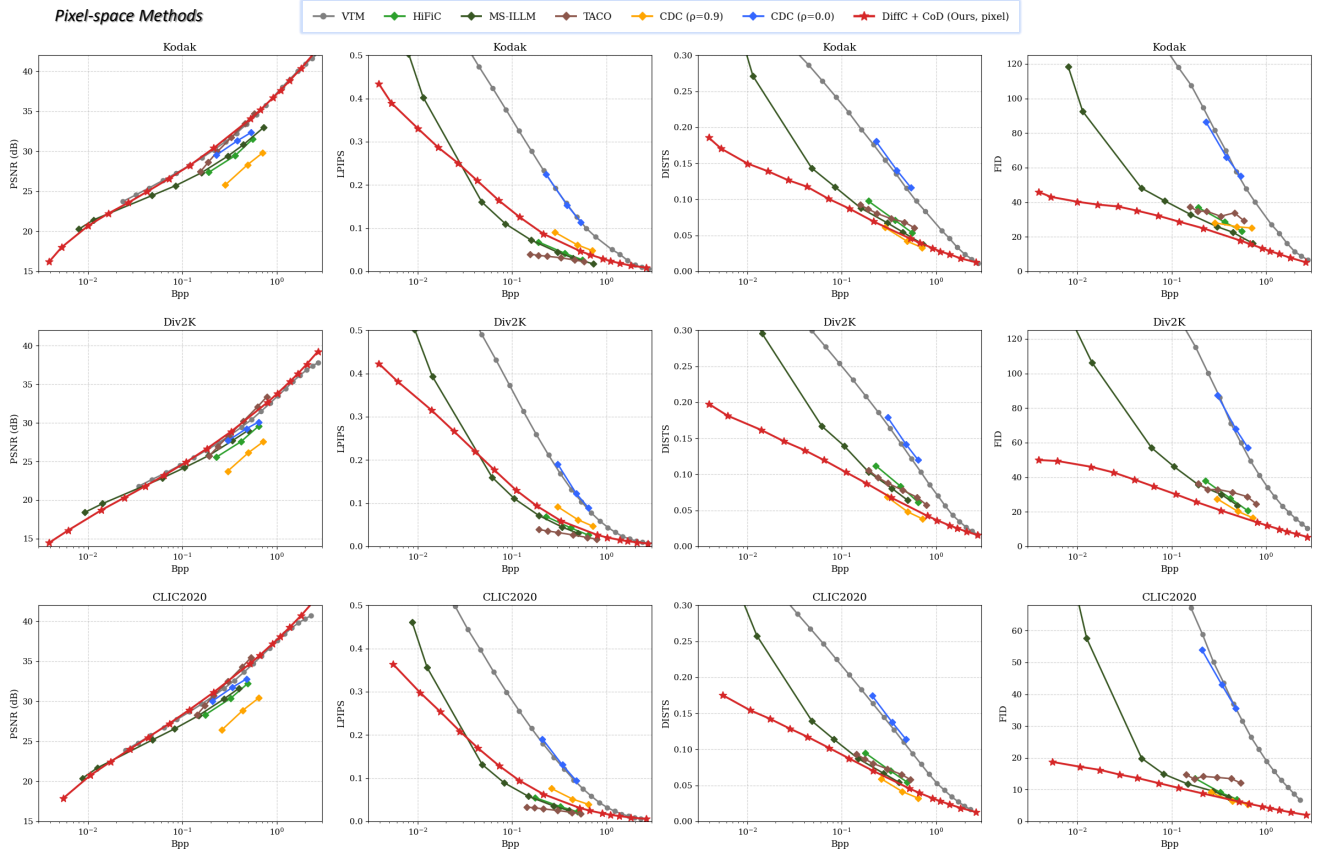


Figure 8. Comparison with pixel-space codecs. *Note: HiFiC, MS-ILLM, CDC, and TACO are optimized using LPIPS, whereas CoD is not. So pixel-space CoD may not achieve the best LPIPS at certain bitrates, despite outperforming in PSNR, DISTS and FID.*

In contrast, HiFiC, MS-ILLM and CDC ( $\rho = 0.9$ ) improve perceptual quality at the expense of PSNR. TACO removes the GAN [14] loss to balance distortion and perception, but fails to achieve an optimal trade-off. By comparison, DiffC with pixel-space CoD attains the best balance across all bitrates. Although pixel diffusion has been less explored than latent diffusion, our results demonstrate that **CoD highlights the potential of pixel diffusion to achieve a superior rate–distortion–perception trade-off.**

**Latent-space Comparison.** The rate-distortion curves on latent space codecs are shown in Figure 9. Compared to existing latent-space codecs, DiffC with latent-space CoD achieves the best reconstruction quality at lower bitrates (e.g.,  $<0.02$  bpp). At higher bitrates, the gap narrows as performance approaches the SD-VAE limit. At some points (e.g., FID at 0.02 bpp on CLIC), CoD performs slightly worse than DiffC due to smaller training scale, which can likely be closed with larger data and training in the future.

**Visualization.** Figure 7 compares visual results across different bitrates among SD-based DiffC, PerCo (SD), and the pixel-space MS-ILLM. At low bitrates, CoD achieves higher fidelity than SD-based codecs and more realistic details than prior pixel-space methods. At high bitrates, latent codecs are

constrained by the reconstruction quality of SD-VAE, e.g., small characters appear heavily distorted, while MS-ILLM also struggles to recover clear text. In contrast, pixel-space CoD reconstructs sharp and accurate details, demonstrating the strong potential of pixel-space diffusion.

## 5. Related Works

### 5.1. Generative Image Compression

Unlike neural image codecs [4, 5, 16] that primarily minimize reconstruction distortion (MSE), generative image compression [2, 3, 17, 23, 24, 52] aims to achieve both low distortion and high perceptual quality. Early works [34, 36] introduced conditional GANs to enhance perceptual realism, successfully improving perceptual quality compared to MSE-optimized codecs, albeit at the cost of higher reconstruction distortion. TACO [28] further incorporates textual information to mitigate MSE degradation, yet still falls short in achieving an ideal distortion–perception balance. To the best of our knowledge, we are the first to demonstrate that pixel-space diffusion can attain VTM-level distortion while delivering superior perceptual quality to GAN-based codecs.

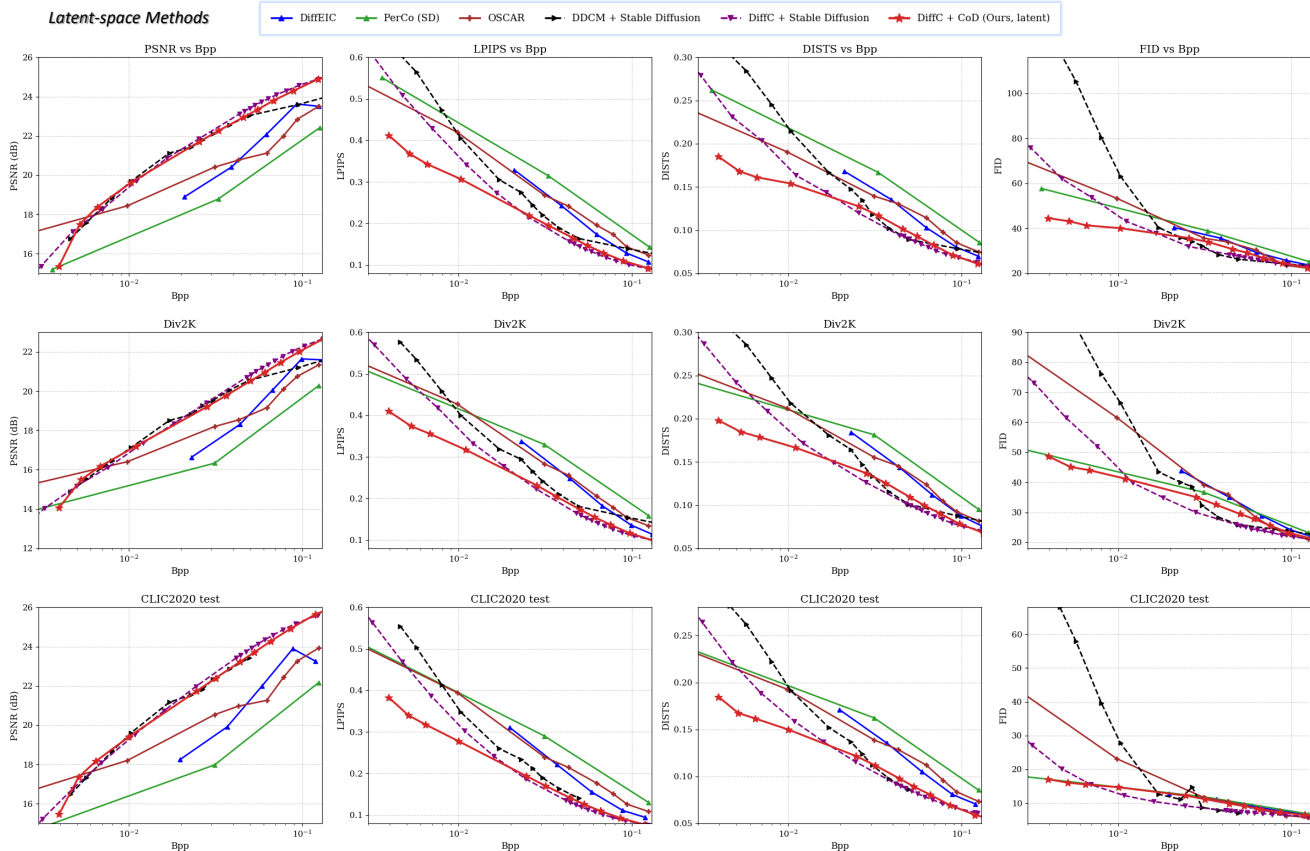


Figure 9. Comparison with latent-space codecs. Latent-space CoD demonstrates state-of-the-art performance towards low bitrates.

## 5.2. Diffusion Image Compression

Recent advances in generative image compression increasingly leverage the powerful generative priors of diffusion models to achieve higher realism. PerCo [7] compresses image representations and text captions as conditions, fine-tuning a pretrained latent diffusion model for perfect realism. In contrast, DiffEIC [32] and OSCAR [15] show that removing the text bitstream can yield better overall performance. Other approaches [11, 51] investigate zero-shot compression using pretrained diffusion models without fine-tuning. DiffC [43, 46] introduces reverse-channel coding to progressively compress increasingly noised representations, while DDCM [37] adopts random codebooks to encode the random sampled noises. Most of these methods depend on pretrained diffusion foundation models such as Stable Diffusion, which are theoretically suboptimal for compression. CoD offers an alternative, compression-oriented diffusion foundation model that can serve as a stronger backbone for such approaches, enabling superior performance.

Another early exploration on pixel-space diffusion codec is CDC [54], which also formulates compression as conditions for diffusion. However, CoD differs in several key aspects. First, CoD emphasizes training at ultra-low bitrates

( $\sim 0.0039$  bpp) to strengthen its strong generative prior, and it relies purely on diffusion loss rather than traditional perceptual losses. In contrast, CDC is trained at high bitrates ( $> 0.2$  bpp), where dense information limits generative learning. Consequently, CDC requires perceptual losses such as LPIPS, otherwise its perceptual quality drops to the level of an MSE-optimized codec. Second, CoD embodies the concept of a foundation codec, scaling training to push the frontier of compression research, while CDC does not consider scaling laws. Finally, CoD offers insights beyond the model itself: we provide a comprehensive analysis of scaling behavior, pixel- vs. latent-space and conditioning modalities, offering broader insights for future research.

## 6. Conclusion and Limitation

To conclude, we present CoD, the first compression-oriented diffusion foundation model. CoD is trained from scratch and enables end-to-end joint optimization of compression and diffusion generation, substantially improving diffusion-based compression performance, particularly at ultra-low bitrates. CoD is trained entirely on open datasets with low computational cost, facilitating reproducibility and further research. Building on CoD, we investigate the scaling laws of

diffusion codecs and demonstrate the potential of pixel-space diffusion towards strong R–D–P trade-off across a wide bitrate range. We believe CoD establishes a solid foundation for future advances in diffusion-based compression.

Despite these advantages, CoD still has several limitations at this stage. First, it is not yet trained for high-resolution inputs. Although extending CoD to higher resolutions (e.g., 2K) is technically feasible, it would require substantially higher computational cost. As an early academic prototype, we leave this for future work. Second, similar to all diffusion codecs, CoD does not meet real-time coding requirements. Nevertheless, as shown in Section 3.2, even a compact CoD model already surpasses GAN-based codecs by a large margin. With continued advances in diffusion distillation, we hope real-time will become attainable in the near future.

## Change Log

- **v1** (2025-11-24): Initial submission.
- **v2** (2025-12-10): Updated algorithms and results for finetuned one-step diffusion codec (App. B), CoD-based perceptual supervision (App. C), analysis on different downstream codecs (App. D), and  $\mathcal{X}$ -prediction (App. E).
- **v3** (2026-03-16): Updated to CVPR camera ready version. Updated Github code link.

## References

- [1] Eirikur Agustsson and Radu Timofte. Ntire 2017 challenge on single image super-resolution: Dataset and study. In *Proceedings of the IEEE conference on computer vision and pattern recognition workshops*, pages 126–135, 2017.
- [2] Eirikur Agustsson, Michael Tschanen, Fabian Mentzer, Radu Timofte, and Luc Van Gool. Generative adversarial networks for extreme learned image compression. In *Proceedings of the IEEE/CVF International Conference on Computer Vision*, pages 221–231, 2019.
- [3] Eirikur Agustsson, David Minnen, George Toderici, and Fabian Mentzer. Multi-realism image compression with a conditional generator. In *Proceedings of the IEEE/CVF Conference on Computer Vision and Pattern Recognition*, pages 22324–22333, 2023.
- [4] Johannes Ballé, Valero Laparra, and Eero P Simoncelli. End-to-end optimized image compression. In *5th International Conference on Learning Representations, ICLR 2017*, 2017.
- [5] Johannes Ballé, David Minnen, Saurabh Singh, Sung Jin Hwang, and Nick Johnston. Variational image compression with a scale hyperprior. In *International Conference on Learning Representations*, 2018.
- [6] Yochai Blau and Tomer Michaeli. Rethinking lossy compression: The rate-distortion-perception tradeoff. In *International Conference on Machine Learning*, pages 675–685. PMLR, 2019.
- [7] Marlene Careil, Matthew J. Muckley, Jakob Verbeek, and Stéphane Lathuilière. Towards image compression with perfect realism at ultra-low bitrates. In *The Twelfth International Conference on Learning Representations*, 2024.
- [8] Junsong Chen, Jincheng YU, Chongjian GE, Lewei Yao, Enze Xie, Zhongdao Wang, James Kwok, Ping Luo, Huchuan Lu, and Zhenguo Li. Pixart- $\alpha$ : Fast training of diffusion transformer for photorealistic text-to-image synthesis. In *The Twelfth International Conference on Learning Representations*, 2024.
- [9] Keyan Ding, Kede Ma, Shiqi Wang, and Eero P Simoncelli. Image quality assessment: Unifying structure and texture similarity. *IEEE transactions on pattern analysis and machine intelligence*, 44(5):2567–2581, 2020.
- [10] Eastman Kodak Company. Kodak lossless true color image suite. <http://r0k.us/graphics/kodak/>, 1999. Accessed: 2025-11-08.
- [11] Noam Elata, Tomer Michaeli, and Michael Elad. PSC: Posterior sampling-based compression. In *15th International Conference on Sampling Theory and Applications*, 2025.
- [12] Patrick Esser, Robin Rombach, and Bjorn Ommer. Taming transformers for high-resolution image synthesis. In *Proceedings of the IEEE/CVF conference on computer vision and pattern recognition*, pages 12873–12883, 2021.
- [13] Marta Gentiloni Silveri, Alain Durmus, and Giovanni Conforti. Theoretical guarantees in kl for diffusion flow matching. *Advances in Neural Information Processing Systems*, 37: 138432–138473, 2024.
- [14] Ian Goodfellow, Jean Pouget-Abadie, Mehdi Mirza, Bing Xu, David Warde-Farley, Sherjil Ozair, Aaron Courville, and Yoshua Bengio. Generative adversarial networks. *Communications of the ACM*, 63(11):139–144, 2020.
- [15] Jinpei Guo, Yifei Ji, Zheng Chen, Kai Liu, Min Liu, Wang Rao, Wenbo Li, Yong Guo, and Yulun Zhang. Oscar: One-step diffusion codec across multiple bit-rates. *arXiv preprint arXiv:2505.16091*, 2025.
- [16] Dailan He, Ziming Yang, Weikun Peng, Rui Ma, Hongwei Qin, and Yan Wang. Elic: Efficient learned image compression with unevenly grouped space-channel contextual adaptive coding. In *Proceedings of the IEEE/CVF Conference on Computer Vision and Pattern Recognition*, pages 5718–5727, 2022.
- [17] Dailan He, Ziming Yang, Hongjiu Yu, Tongda Xu, Jixiang Luo, Yuan Chen, Chenjian Gao, Xinjie Shi, Hongwei Qin, and Yan Wang. Po-elic: Perception-oriented efficient learned image coding. In *Proceedings of the IEEE/CVF Conference on Computer Vision and Pattern Recognition*, pages 1764–1769, 2022.
- [18] Kaiming He, Xiangyu Zhang, Shaoqing Ren, and Jian Sun. Deep residual learning for image recognition. In *Proceedings of the IEEE conference on computer vision and pattern recognition*, pages 770–778, 2016.
- [19] Martin Heusel, Hubert Ramsauer, Thomas Unterthiner, Bernhard Nessler, and Sepp Hochreiter. Gans trained by a two time-scale update rule converge to a local nash equilibrium. *Advances in neural information processing systems*, 30, 2017.
- [20] Jonathan Ho and Tim Salimans. Classifier-free diffusion guidance. In *NeurIPS 2021 Workshop on Deep Generative Models and Downstream Applications*, 2021.

- [21] Jonathan Ho, Ajay Jain, and Pieter Abbeel. Denoising diffusion probabilistic models. *Advances in neural information processing systems*, 33:6840–6851, 2020.
- [22] Edward J Hu, Yelong Shen, Phillip Wallis, Zeyuan Allen-Zhu, Yuanzhi Li, Shean Wang, Lu Wang, Weizhu Chen, et al. Lora: Low-rank adaptation of large language models. *ICLR*, 1(2):3, 2022.
- [23] Shoma Iwai, Tomo Miyazaki, Yoshihiro Sugaya, and Shinichiro Omachi. Fidelity-controllable extreme image compression with generative adversarial networks. In *2020 25th International Conference on Pattern Recognition (ICPR)*, pages 8235–8242. IEEE, 2021.
- [24] Zhaoyang Jia, Jiahao Li, Bin Li, Houqiang Li, and Yan Lu. Generative latent coding for ultra-low bitrate image compression. In *Proceedings of the IEEE/CVF Conference on Computer Vision and Pattern Recognition*, pages 26088–26098, 2024.
- [25] Alexander Kirillov, Eric Mintun, Nikhila Ravi, Hanzi Mao, Chloe Rolland, Laura Gustafson, Tete Xiao, Spencer Whitehead, Alexander C Berg, Wan-Yen Lo, et al. Segment anything. In *Proceedings of the IEEE/CVF international conference on computer vision*, pages 4015–4026, 2023.
- [26] Alina Kuznetsova, Hassan Rom, Neil Alldrin, Jasper Uijlings, Ivan Krasin, Jordi Pont-Tuset, Shahab Kamali, Stefan Popov, Matteo Mallocci, Alexander Kolesnikov, et al. The open images dataset v4: Unified image classification, object detection, and visual relationship detection at scale. *International journal of computer vision*, 128(7):1956–1981, 2020.
- [27] Nikolai Körber, Eduard Kromer, Andreas Siebert, Sascha Hauke, Daniel Mueller-Gritschneider, and Björn W. Schuller. Perco (sd): Open perceptual compression. *CoRR*, 2024.
- [28] Hagyeong Lee, Minkyu Kim, Jun-Hyuk Kim, Seungeon Kim, Dokwan Oh, and Jaeho Lee. Neural image compression with text-guided encoding for both pixel-level and perceptual fidelity. In *International Conference on Machine Learning*, 2024.
- [29] Eric Lei, Yigit Berkay Uslu, Hamed Hassani, and Shirin Saeedi Bidokhti. Text + sketch: Image compression at ultra low rates. In *ICML 2023 Workshop Neural Compression: From Information Theory to Applications*, 2023.
- [30] Junnan Li, Dongxu Li, Silvio Savarese, and Steven Hoi. Blip-2: Bootstrapping language-image pre-training with frozen image encoders and large language models. In *International conference on machine learning*, pages 19730–19742. PMLR, 2023.
- [31] Tianhong Li and Kaiming He. Back to basics: Let denoising generative models denoise. *arXiv preprint arXiv:2511.13720*, 2025.
- [32] Zhiyuan Li, Yanhui Zhou, Hao Wei, Chenyang Ge, and Jingwen Jiang. Towards extreme image compression with latent feature guidance and diffusion prior. *IEEE Transactions on Circuits and Systems for Video Technology*, 2024.
- [33] Xingchao Liu, Chengyue Gong, and qiang liu. Flow straight and fast: Learning to generate and transfer data with rectified flow. In *The Eleventh International Conference on Learning Representations*, 2023.
- [34] Fabian Mentzer, George D Toderici, Michael Tschannen, and Eirikur Agustsson. High-fidelity generative image compression. *Advances in neural information processing systems*, 33: 11913–11924, 2020.
- [35] Fabian Mentzer, David Minnen, Eirikur Agustsson, and Michael Tschannen. Finite scalar quantization: VQ-VAE made simple. In *The Twelfth International Conference on Learning Representations*, 2024.
- [36] Matthew J Muckley, Alaeldin El-Nouby, Karen Ullrich, Hervé Jégou, and Jakob Verbeek. Improving statistical fidelity for neural image compression with implicit local likelihood models. In *International Conference on Machine Learning*, pages 25426–25443. PMLR, 2023.
- [37] Guy Ohayon, Hila Manor, Tomer Michaeli, and Michael Elad. Compressed image generation with denoising diffusion codebook models. In *Forty-second International Conference on Machine Learning*, 2025.
- [38] Maxime Oquab, Timothée Darcet, Théo Moutakanni, Huy Vo, Marc Szafraniec, Vasil Khalidov, Pierre Fernandez, Daniel Haziza, Francisco Massa, Alaeldin El-Nouby, et al. DINOv2: Learning robust visual features without supervision. *Transactions on Machine Learning Research*, 2024.
- [39] Robin Rombach, Andreas Blattmann, Dominik Lorenz, Patrick Esser, and Björn Ommer. High-resolution image synthesis with latent diffusion models. In *Proceedings of the IEEE/CVF conference on computer vision and pattern recognition*, pages 10684–10695, 2022.
- [40] Olga Russakovsky, Jia Deng, Hao Su, Jonathan Krause, Sanjeev Satheesh, Sean Ma, Zhiheng Huang, Andrej Karpathy, Aditya Khosla, Michael Bernstein, et al. Imagenet large scale visual recognition challenge. *International journal of computer vision*, 115(3):211–252, 2015.
- [41] Tim Salimans and Jonathan Ho. Progressive distillation for fast sampling of diffusion models. *arXiv preprint arXiv:2202.00512*, 2022.
- [42] Yang Song and Stefano Ermon. Generative modeling by estimating gradients of the data distribution. *Advances in neural information processing systems*, 32, 2019.
- [43] Lucas Theis, Tim Salimans, Matthew D Hoffman, and Fabian Mentzer. Lossy compression with gaussian diffusion. *arXiv preprint arXiv:2206.08889*, 2022.
- [44] George Toderici, Lucas Theis, Nick Johnston, Eirikur Agustsson, Fabian Mentzer, Johannes Ballé, Wenzhe Shi, and Radu Timofte. Clic 2020: Challenge on learned image compression. *Retrieved March*, 29:2021, 2020.
- [45] Ashish Vaswani, Noam Shazeer, Niki Parmar, Jakob Uszkoreit, Llion Jones, Aidan N Gomez, Łukasz Kaiser, and Illia Polosukhin. Attention is all you need. *Advances in neural information processing systems*, 30, 2017.
- [46] Jeremy Vonderfecht and Feng Liu. Lossy compression with pretrained diffusion models. In *The Thirteenth International Conference on Learning Representations*, 2025.
- [47] VVC-21.2. [https://vcgit.hhi.fraunhofer.de/jvet/VVCSsoftware\\_VTM/-/tree/VTM-21.2](https://vcgit.hhi.fraunhofer.de/jvet/VVCSsoftware_VTM/-/tree/VTM-21.2). Accessed: 10/23/2023, 2023.
- [48] Shuai Wang, Ziteng Gao, Chenhui Zhu, Weilin Huang, and Limin Wang. Pixnerd: Pixel neural field diffusion. *arXiv preprint arXiv:2507.23268*, 2025.

- [49] Shuai Wang, Zhi Tian, Weilin Huang, and Limin Wang. Ddt: Decoupled diffusion transformer. *arXiv preprint arXiv:2504.05741*, 2025.
- [50] Tongda Xu. Optimizing input of denoising score matching is biased towards higher score norm. *arXiv preprint arXiv:2511.11727*, 2025.
- [51] Tongda Xu, Ziran Zhu, Dailan He, Yanghao Li, Lina Guo, Yuanyuan Wang, Zhe Wang, Hongwei Qin, Yan Wang, Jingjing Liu, and Ya-Qin Zhang. Idempotence and perceptual image compression. In *The Twelfth International Conference on Learning Representations*, 2024.
- [52] Naifu Xue, Zhaoyang Jia, Jiahao Li, Bin Li, Yuan Zhang, and Yan Lu. Df: Extreme image compression with dual-generative latent fusion. In *Proceedings of the IEEE/CVF International Conference on Computer Vision (ICCV)*, 2025.
- [53] Naifu Xue, Zhaoyang Jia, Jiahao Li, Bin Li, Yuan Zhang, and Yan Lu. One-step diffusion-based image compression with semantic distillation. In *The Thirty-ninth Annual Conference on Neural Information Processing Systems*, 2025.
- [54] Ruihan Yang and Stephan Mandt. Lossy image compression with conditional diffusion models. *Advances in Neural Information Processing Systems*, 36:64971–64995, 2023.
- [55] Tianwei Yin, Michaël Gharbi, Richard Zhang, Eli Shechtman, Fredo Durand, William T Freeman, and Taesung Park. One-step diffusion with distribution matching distillation. In *Proceedings of the IEEE/CVF conference on computer vision and pattern recognition*, pages 6613–6623, 2024.
- [56] Sihyun Yu, Sangkyung Kwak, Huiwon Jang, Jongheon Jeong, Jonathan Huang, Jinwoo Shin, and Saining Xie. Representation alignment for generation: Training diffusion transformers is easier than you think. In *The Thirteenth International Conference on Learning Representations*, 2025.
- [57] Richard Zhang, Phillip Isola, Alexei A Efros, Eli Shechtman, and Oliver Wang. The unreasonable effectiveness of deep features as a perceptual metric. In *Proceedings of the IEEE conference on computer vision and pattern recognition*, pages 586–595, 2018.
- [58] Tianyu Zhang, Xin Luo, Li Li, and Dong Liu. Stablecodec: Taming one-step diffusion for extreme image compression. In *Proceedings of the IEEE/CVF International Conference on Computer Vision (ICCV)*, pages 17379–17389, 2025.

## Appendices

This document provides the supplementary material to **Compression-oriented Diffusion foundation model, CoD**. Beyond additional training details and extended results, we further investigate its characteristics and explore additional downstream codec applications.

The key conclusions are summarized below:

- **Extreme 64-bit compression:** CoD compresses image into only 64 bits while preserving correct semantics.
- **One-step diffusion codec:** Finetuning one-step CoD achieves real-time and SOTA performance, comparable to StableCodec [58] and OneDC [53].
- **CoD as perceptual loss:** CoD-based perceptual loss significantly improves MS-ILLM [36].
- **$\mathcal{X}$ -prediction advantage:** Using  $\mathcal{X}$ -prediction yields better performance than  $\mathcal{V}$ -prediction for CoD (pixel).

### A. Towards 64-Bit Image Compression

In this paper, we primarily discuss CoD at 0.0039 bpp, which corresponds to 1024 bits for a  $512 \times 512$  image. Results demonstrate that the shape, color, and high-level semantic fidelity are well preserved under this bitrate. In this section, we further explore a more extreme compression of 64 bits for a  $512 \times 512$  image (i.e., 0.00024 bpp) to analyze the boundary of semantic-level compression. To achieve 64 bits, our encoder downsamples the original image to  $1/128$  of its original resolution ( $4 \times 4$  patches) and uses a codebook size of  $2^4 = 16$ . Since latent-space CoD performs better at lower bitrates (Figure 5 in the paper), we train our 64-bit CoD on latent space.



Figure 10. Evaluation of 64-bit CoD on Kodak at  $512 \times 512$ .

We evaluate our 64-bit CoD on the Kodak dataset in Figure 10. Surprisingly, under such an extremely low bitrate,

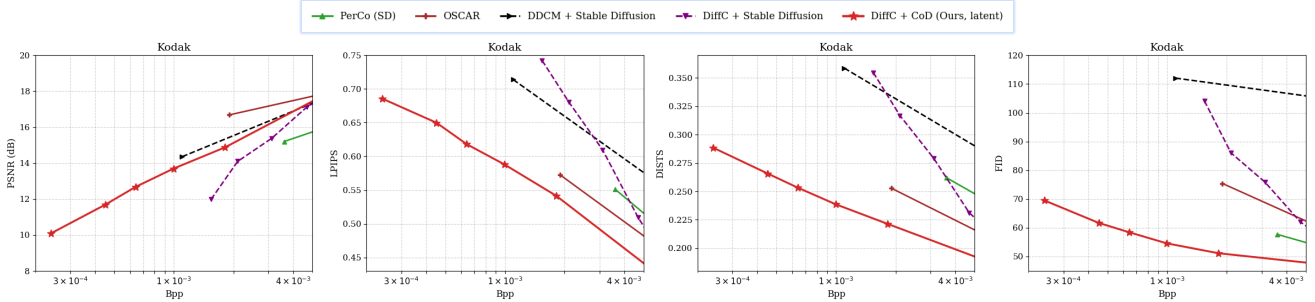


Figure 11. Rate-Distortion curves for 64-bit CoD and Stable Diffusion based codecs on Kodak at  $512 \times 512$ .

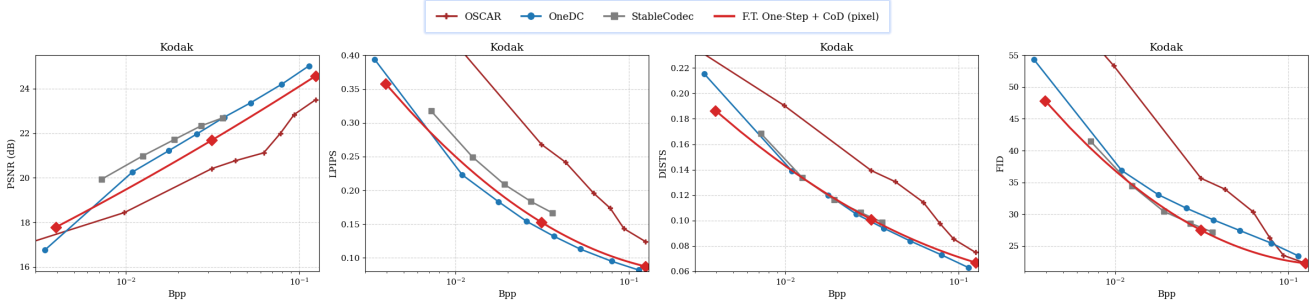


Figure 12. Rate-Distortion curves for finetuned one-step CoD and other one-step diffusion codecs on Kodak at  $512 \times 512$ .

CoD successfully reconstructs the correct semantics of the original image. By contrast, Stable Diffusion based codecs DDCM [37] and DiffC [46] fail to reconstruct correct semantics even at a fourfold ( $4\times$ ) higher bit cost. We further leverage DiffC to evaluate the downstream compression performance on Kodak [10] in Figure 11, where CoD-based DiffC significantly outperforms other Stable Diffusion based codecs. Our scheme achieves a FID of 70 with only less than 10% of the bits of prior codecs, highlighting the extreme compression capability of 64-bit CoD.

arately, one-step diffusion can be trained end-to-end, enabling better overall performance. OSCAR [15] fine-tuned a multi-step Stable Diffusion to function as a one-step image codec. StableCodec [58] leverages a one-step SD-Turbo as the foundation model, achieving significantly improved performance. Similarly, OneDC [53] employs a one-step DMD-distilled [55] Stable Diffusion as the foundation model for one-step diffusion compression. The success of these approaches motivates our exploration of CoD in the context of one-step diffusion foundation models.



Figure 13. Evaluation of one-step CoD on Kodak at  $512 \times 512$ .

## B. Towards One-Step Diffusion Compression

### B.1. Preliminary

Recently, one-step diffusion models have demonstrated effectiveness in generative image compression. Unlike multi-step diffusion, which optimizes each diffusion timestep sep-

arately, one-step diffusion can be trained end-to-end, enabling better overall performance. OSCAR [15] fine-tuned a multi-step Stable Diffusion to function as a one-step image codec. StableCodec [58] leverages a one-step SD-Turbo as the foundation model, achieving significantly improved performance. Similarly, OneDC [53] employs a one-step DMD-distilled [55] Stable Diffusion as the foundation model for one-step diffusion compression. The success of these approaches motivates our exploration of CoD in the context of one-step diffusion foundation models.

$$\nabla_{\theta} D_{KL} = \mathbb{E}_{z \sim \mathcal{N}(0; \mathbf{I})} \left[ - (s_{\text{real}}(x) - s_{\text{fake}}(x)) \frac{dG}{d\theta} \right], \quad (9)$$

where  $s_{\text{real}}(x)$  and  $s_{\text{fake}}(x)$  are the score functions [42] of their respective distributions. By adding random noise to  $x$ , the score can be predicted by a diffusion model. DMD leverages a pretrained multi-step diffusion model for the real score and dynamically trains a diffusion model to estimate the fake score for one-step samples  $x$ .

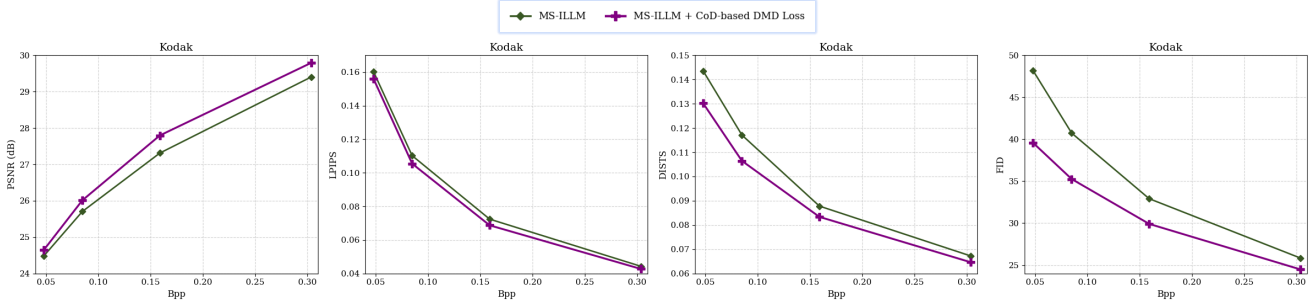


Figure 14. Rate-Distortion curves for MS-ILLM [36] and finetuning MS-ILLM decoder with CoD-based DMD loss on Kodak at  $512 \times 512$ .

## B.2. Distilling a CoD

We train a one-step CoD using a combination of losses and multi-step CoD-based DMD loss:

$$\mathcal{L}_{OS} = \mathcal{L}_{\text{pixel}} + \mathcal{L}_{\text{perc}} + \lambda \cdot \mathcal{L}_{\text{REPA}} + \beta \cdot \mathcal{L}_C, \quad (10)$$

where  $L_{\text{pixel}} = \mathcal{L}_1 + \mathcal{L}_{\text{LPIPS}}$  consists of pixel-space L1 loss and the LPIPS [57] loss,  $L_{\text{perc}} = 2 \cdot \mathcal{L}_{\text{DMD}} + 0.01 \cdot \mathcal{L}_{\text{GAN}}$  consists of a DMD loss and a patch GAN loss [12],  $\mathcal{L}_{\text{REPA}}$  is the representation alignment loss and  $\mathcal{L}_C$  is th codebook commitment loss. We set  $\lambda = 0.5$  and  $\beta = 0.25$ .

For simplicity, we optimize only the pixel-space CoD, allowing pixel-space losses to be computed directly. Following the DMD procedure, we update the one-step CoD every 10 steps, while the remaining 9 steps train the fake score diffusion model. The model is trained for 100K steps (i.e., 10K steps for the one-step CoD) with a batch size of 32, which takes approximately 96 A100 GPU hours in total, which is much less than 1664 A100 GPU hours of DMD-based Stable Diffusion distillation. The learning rates for one-step CoD and fake score network are set to  $10^{-5}$ .

## B.3. Finetuning to Higher Bitrates

In the previous section, we distilled the one-step CoD model at 0.0039 bpp. We further observe that the distilled model can be efficiently adapted to higher bitrates. Following PerCo and OSCAR, we adjust both the downsampling scale in the condition encoder and the codebook size according to the target bitrate. Specifically, we train two variants: 0.0312 bpp with  $16 \times$  downsampling and codebook size 256, and 0.125 bpp with  $8 \times$  downsampling and codebook size 256.

**Stage I: initialization.** We randomly set the parameters of the condition encoder, codebook, and condition decoder, while loading the pre-trained multi-step CoD weights for the diffusion module. During this warm-up phase, the diffusion module is trained using LoRA [22] with rank 32. To accelerate convergence, we remove the  $L_{\text{perc}}$  term from  $L_{OS}$  and train for 200K steps with a learning rate of  $10^{-4}$ .

**Stage II: Fine-tuning.** We then fine-tune all model components jointly using the full  $L_{OS}$  for another 100K steps with a batch size of 32 and a learning rate of  $10^{-5}$ . With perceptual

supervision restored, the fine-tuned one-step CoD achieves significantly improved performance at higher bitrates.

## B.4. Evaluation

**Comparison with one-step codecs.** We evaluate the fine-tuned one-step CoD on the Kodak dataset (Figure 12). It yields competitive reconstruction quality compared with SOTA one-step diffusion codecs such as OneDC and StableCodec, particularly at ultra-low bitrates. Notably, our method does not rely on any pretrained components from Stable Diffusion (e.g., one-step models or SD-VAEs) to reach this performance. We currently adopt fixed-length coding for the codebook indices for simplicity. Further gains can be achieved by introducing an entropy model or applying latent compression [24]. Visual comparisons in Figure 13 further show that one-step CoD preserves higher fidelity than both multi-step CoD and OneDC.

**Complexity Analysis.** DiT injects conditions and timesteps through AdaLN-Zero layers, which account for more than 200M parameters in CoD. However, CoD concatenates compression conditions directly with the noised input along the channel dimension instead of injecting them through AdaLN-Zero (see Section 2.1). Under the one-step setting, the timestep is fixed to 0, making all AdaLN-Zero outputs constant and therefore redundant. Thus, we precompute these constants and remove the AdaLN-Zero modules to further reduce computation and memory access. As shown in Table 4, one-step CoD processes a  $512 \times 512$  image in only 25.2 ms, which is even faster than a single step of Stable Diffusion used in OneDC and StableCodec. This demonstrates its potential in real-time application.

## C. Towards Perceptual Supervision via CoD

In the DMD loss in Equation 9, for any input  $x$ , we can optimize its KL divergence using CoD to estimate real and fake scores. This indicates that CoD can act as a perceptual supervision mechanism, enhancing the realism of reconstructions for a variety of networks, including other pixel-space codecs, restoration models, or super-resolution models. To demonstrate this potential, we finetune the pixel-space codec MS-ILLM [36] using the CoD-based DMD loss.

Methods	PSNR	LPIPS	DISTS	FID
MS-ILLM	<b>21.43 dB</b>	0.403	0.271	92.5
+ CoD-based DMD loss	21.08 dB	<b>0.376</b>	<b>0.248</b>	<b>80.92</b>

Table 1. Finetuning the decoder of MS-ILLM using CoD as a perceptual supervision. Evaluated on Kodak at  $512 \times 512$ . BPP=0.011.



Figure 15. Finetuning MS-ILLM decoder with CoD-based DMD loss.

**Evaluation.** MS-ILLM is typically pretrained using the MSE loss, after which the encoder and entropy model are fixed while the decoder is finetuned with perceptual losses such as LPIPS and GAN [14] loss. Following this paradigm, we finetune only the decoder of MS-ILLM, replacing the GAN loss with the CoD-based DMD loss. Remarkably, after optimizing the decoder for just 2K steps with a batch size of 32 (20K steps total including fake score learning), MS-ILLM demonstrates substantially improved perceptual quality across all metrics, as shown in Figure 14. Towards ultra-low bitrates like 0.011 bpp where the information is severely distorted, we find increasing the learning rate of fake score network training can better capture the distorted distribution to enhance realism, as shown in Table 1. Several visual examples are presented in Figure 15, where the CoD-based DMD loss markedly reduces artifacts and yields clearer edges and finer details. Since the encoder is fixed, the encoded information remains heavily distorted under MSE-only optimization, resulting in poor overall reconstruction. We expect that jointly tuning the entire network with the CoD-based DMD loss could further improve perceptual quality.

**Discussion.** Instead of relying on text conditions, CoD learns native image conditions for diffusion. Under DMD supervision, conditions are important since they guide which types

of realistic details to generate. Native image conditions provide directions that more closely align with the original image, making CoD theoretically better suited as DMD supervision for reconstruction-related tasks. Moreover, CoD is text-free, eliminating the need for extensive captioning at each optimization step and thereby improving training efficiency. In addition, adopting latent diffusion for DMD loss is non-trivial for pixel-space codecs, whereas our pixel-space CoD offers a more direct and compatible solution.

## D. Analysis on Different Downstream Codecs

In this section, we further demonstrate the capability of CoD as a foundation model through comparing different downstream codecs in Figure 16.

### D.1. Comparison of Downstream Codecs

**Zero-shot DiffC.** No perceptual optimization is involved. It yields the highest PSNR and strong perceptual quality, but has slow encoding speed. Runtime grows with bitrate, and encoding a 4 bpp image can take up to 100 seconds.

**Finetuned one-step CoD.** This scheme attains the best perceptual scores, especially DISTS and FID. The single-step diffusion process enables very fast encoding. However, end-to-end perceptual finetuning with perceptual losses leads to relatively lower PSNR.

**CoD-based perceptual optimization for MS-ILLM.** Although slightly worse than zero-shot DiffC, it requires a lightweight model and offers substantially faster coding, providing a different balance between coding speed and compression ratio.

### D.2. Finetuning Multi-step CoD at Higher Bitrates

A straightforward downstream compression scheme is to directly finetune multi-step CoD at higher bitrates through diffusion loss. However, this leads to inferior results compared to other schemes. When jointly optimizing a condition under explicit diffusion loss, the optimization becomes biased: the condition tends to maximize the score norm, as shown in [50]. In practice, this drives the decoder toward oversharpened and over-saturated reconstructions, resulting in lower fidelity. This observation is consistent with recent findings that one-step diffusion codecs perform better because they avoid this biased optimization.

The tendency toward a higher score norm also motivates training the foundation model at ultra-low bitrates. Under a strong information bottleneck, the condition can only preserve a small amount of information. The distortion is large at these rates, forcing the available condition to focus on reducing diffusion loss rather than amplifying the score norm. At higher bitrates, reducing diffusion loss becomes easier, leaving room for the condition to optimize for score norm instead. In addition, our unified training strategy and aux-

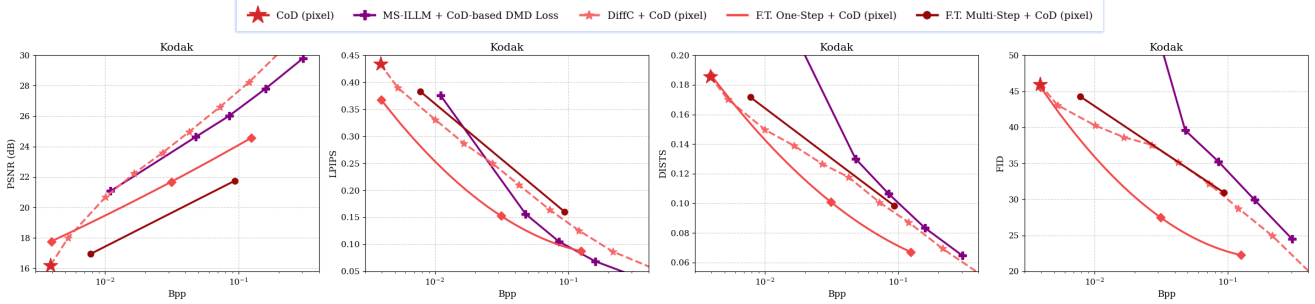


Figure 16. Rate-Distortion curves for different downstream codecs built on pixel-space CoD on Kodak at  $512 \times 512$ .

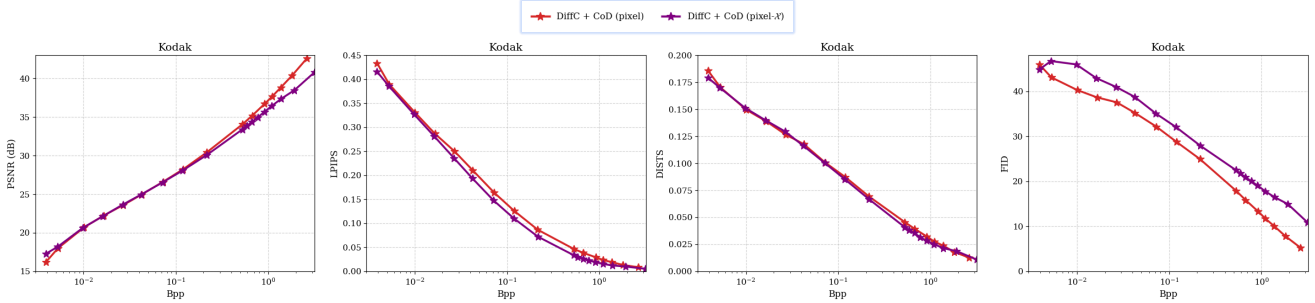


Figure 17. Evaluating  $\mathcal{V}$ - and  $\mathcal{X}$ -prediction pixel-space CoD using DiffC on Kodak at  $512 \times 512$ .

iliary losses further help counteract this bias by providing additional compression supervision to the condition network.

## E. Exploring $\mathcal{X}$ -Prediction Pixel Diffusion

Since  $\mathcal{V}$ -prediction (velocity prediction) was proposed [41] and later adopted by Stable Diffusion v2.1, it has become a common practice in latent diffusion models, including the baseline diffusion architectures used in our work [48, 49]. However, recent research by Just Image Diffusion (JiT) [31] shows that pixels lie on a low-dimensional manifold, making  $\mathcal{X}$ -prediction a more effective approach for directly modeling pixel distributions. In this paper, we primarily adopt  $\mathcal{V}$ -prediction to provide a unified view of latent- and pixel-space compression. Nevertheless, in this section, we conduct experiments to demonstrate that  $\mathcal{X}$ -prediction can achieve better reconstruction performance.

Method @ 0.0039 bpp	PSNR	LPIPS	DISTS	FID
CoD (pixel)	16.21 dB	0.434	0.186	46.0
CoD (pixel- $\mathcal{X}$ )	<b>17.29 dB</b>	<b>0.416</b>	<b>0.179</b>	<b>44.8</b>
CoD (pixel- $\mathcal{X}$ , JiT)	16.89 dB	0.422	0.183	47.4

Table 2. Ablation study for  $\mathcal{X}$ -prediction on Kodak at  $512 \times 512$ .

**Comparison on pixel-space CoD.** We follow the JiT training pipeline to build a pixel-space CoD variant using  $\mathcal{X}$ -prediction and  $\mathcal{V}$ -loss, denoted as CoD (pixel- $\mathcal{X}$ ) to distinguish it from our velocity-based pixel-space CoD. To further examine the influence of network design (i.e., the decoupled

head [48, 49]) we also substitute our pixel-space diffusion model with JiT’s DiT backbone, referred to as CoD (pixel- $\mathcal{X}$ , JiT). As shown in Table 2,  $\mathcal{X}$ -prediction yields significantly better perceptual metrics than  $\mathcal{V}$ -prediction. In contrast, replacing the decoupled-head design with JiT’s pure DiT structure does not provide performance gains.

**Evaluation on downstream DiffC.** In Figure 17, we evaluate CoD (pixel- $\mathcal{X}$ ) on the downstream codec DiffC. Although  $\mathcal{X}$ -prediction improves performance on the foundation model, it does not consistently benefit DiffC. This is because converting the predicted  $x$  into velocity  $v$  at time  $t$  requires clamping the denominator to be no smaller than 0.05 for stability (following JiT):  $v = (x - x_t) / \text{clamp}(1 - t, 0.05, 1)$ . This clamping leads to inaccurate likelihood estimation near  $t = 1$ . When applied to DiffC, the resulting reconstructions retain slight noisy, i.e., the inversion process does not fully denoise the image, leading to degraded FID. The effect is more pronounced at very high bitrates, where the inaccurate likelihood directly impacts DiffC and causes all metrics to drop relative to  $\mathcal{V}$ -prediction. These results highlight that different prediction targets offer different strengths, and the choice should be adapted to the task objective.

## F. Additional Details and Results

This section provides further training details and additional evaluation results, including complexity analysis, additional evaluation metrics and visual comparisons.

Method	Stage	Image Resolution	BPP / Total Bits	#Images	Training Steps	Batch Size	Learning Rate	GPU hours (A100)
CoD	Low-Resolution Pre-Training	256 × 256	0.0156 bpp / 1024 bits	22.1M	400 K	4 × 32	1 × 10 <sup>-4</sup>	4 × 67
CoD	High-Resolution Pre-Training	512 × 512	0.0039 bpp / 1024 bits	12.8 M	100 K	4 × 16	2 × 10 <sup>-5</sup>	4 × 25
CoD	Unified Post-Training	512 × 512	0.0039 bpp / 1024 bits	12.8 M	50 K	4 × 16	2 × 10 <sup>-5</sup>	4 × 24

Table 3. Detailed configuration of each CoD training stage. The full training process takes 464 A100 GPU hours (approximately 20 days).

Speed (ms) / Params.	Per-Module Breakdown			Steps	Total
	Conditioner	Diffusion	VAE Decoder		
Stable Diffusion v1.5	203.0 / 3.7 B*	30.6 / 860 M	43.4 / 49 M	25	1011 / 4.6 B
Latent-space CoD	8.3 / 177 M	21.5 / 676 M	43.4 / 49 M	25	589.2 / 901 M
Pixel-space CoD	8.3 / 177 M	25.5 / 720 M	- / -	25	645.8 / 897 M
One-Step Pixel-space CoD	8.3 / 177 M	16.9 / 513 M**	- / -	1	25.2 / 690 M

\* Using BLIP2 captioner with at most 32 tokens, as suggested by PerCo (SD) [27].

\*\* The AdaLN-Zero layers are omitted since they become redundant when inference operates with a fixed  $t = 0$ .

Table 4. Complexity comparison with Stable Diffusion. Average speed (ms) is measured for 512 × 512 on A100.

ID	Ablation @ 0.0039 bpp	PSNR	LPIPS	FID
A	Flow matching loss	9.83 dB	0.576	76.8
B	A + Auxiliary Loss	15.20 dB	0.458	48.3
C	A + Unified Training	15.83 dB	0.433	48.4
D	B + Unified Post-Training	<b>16.20 dB</b>	<b>0.433</b>	<b>46.0</b>

Table 5. Ablation study on unified training and auxiliary loss on Kodak at 512 × 512.

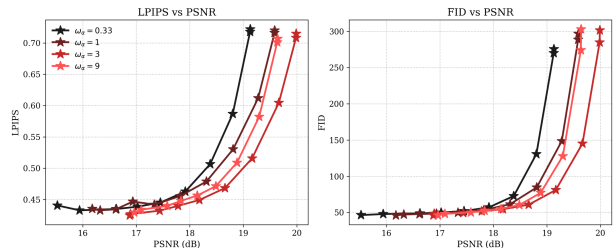


Figure 18. Ablation study on  $\omega_\alpha$  in unified post-training.

## F.1. Training Details

### F.1.1 Datasets

We train the model using three publicly available datasets: **ImageNet-21K** [40] contains 14.2M images across 21K categories. After removing images with a shorter edge below 256 pixels, 9.3M images remain for 256 × 256 pre-training. **OpenImages** [26] and **SA-1B** [25] provide high-resolution images. We use 1.7M directly downloadable images from OpenImages V4 and all 11.1M images from SA-1B for both 256 × 256 and 512 × 512 resolution pre-training. Overall, CoD is trained on 22.1M images. Compared with modern diffusion pipelines, this is a relatively modest data scale, and the only filtering criterion is image resolution rather than extensive data cleaning. We expect that scaling up training with higher-quality data will further improve the performance of CoD.

### F.1.2 Unified Training

Section 2.2 (in the paper) emphasizes that unified training is crucial for achieving high reconstruction fidelity. Table 5 reinforces this observation: unified training (ID = C) provides a clear improvement over the baseline (ID = A). Without unified optimization of the condition and diffusion branches, the condition model tends to encode only structural infor-

mation while neglecting essential color cues. An intuitive workaround is to impose explicit supervision on the condition learning using an auxiliary loss  $\mathcal{L}_{\text{aux}}$ .

**Auxiliary Loss.** Given the output of the condition decoder, we attach two lightweight auxiliary prediction heads to (1) reconstruct the input  $x$  and (2) predict its DINO v2 [38] representation. The auxiliary objective is

$$\mathcal{L}_{\text{aux}} = \mathcal{L}_{\text{aux}}^{\text{MSE}} + 0.5 \cdot \mathcal{L}_{\text{aux}}^{\text{DINO}} \quad (11)$$

where  $\mathcal{L}_{\text{aux}}^{\text{MSE}}$  measures pixel reconstruction accuracy, and  $\mathcal{L}_{\text{aux}}^{\text{DINO}}$  promotes feature consistency by maximizing the cosine similarity between predicted and ground-truth DINO representations. Each auxiliary head consists of a lightweight three-layer convolutional module, adding negligible training overhead. All auxiliary heads are removed at inference time. As shown in Table 5, auxiliary supervision alone (ID = B) achieves FID competitive with unified training, but exhibits lower PSNR and LPIPS since the diffusion model does not receive direct distortion supervision.

**Unified Post-Training.** Motivated by the complementary strengths of unified training and auxiliary supervision, we combine both approaches to further improve performance. Specifically, we first pre-train CoD with auxiliary loss and then post-train it using unified training. For simplicity, rather than randomly selecting a subset of  $\alpha\%$  samples for one-step

Metric	PerCo	OSCAR	DiffC	DDCM	OneDC	CoD
User Score (1-5) $\uparrow$	3.3	2.0	1.8	1.6	3.4	<b>4.2</b>
CLIP Sim. $\uparrow$	0.84	0.78	0.72	0.63	0.84	<b>0.89</b>
Caption Sim. $\uparrow$	0.87	0.83	0.76	0.72	0.86	<b>0.89</b>
VQA Acc. $\uparrow$	69%	66%	58%	48%	71%	<b>80%</b>

Table 6. Additional evaluation metrics including user study and semantic scores around 0.004 bpp on Kodak.

training, we apply a unified objective to all samples during post-training:  $\mathcal{L}_{\text{RF}} = \omega_{\alpha} \cdot \mathcal{L}_{\text{RF}}^{\text{one-step}} + \mathcal{L}_{\text{RF}}^{\text{multi-step}}$ , where  $\omega_{\alpha}$  serves as a weighting factor for the one-step loss component. This brings a little better performance. As shown in Table 5, this unified post-training strategy (ID = D) achieves the best overall results among all configurations.

We adopt  $\omega_{\alpha} = 1$  as the default setting for unified post-training. In Figure 18, we conduct a sensitivity analysis of this parameter, and the results demonstrate that a value of  $\omega_{\alpha} = 3$  yields additional performance gains, suggesting that further optimization of this hyperparameter could enhance overall efficacy.

### F.1.3 Multi-Stage Training

In Table 3, we summarize the configuration of all CoD training stages. A key design choice is to keep the total amount of transmitted information fixed across different resolutions. Concretely, we allocate 0.0156 bpp at 0.0156 bpp at  $256 \times 256$  and 0.0039 bpp at  $512 \times 512$ , which correspond to the same total bottleneck size of 1024 bits. The codebook size remains unchanged across resolutions. Instead, we change the downsample ratio in the encoder, i.e.,  $16\times$  at  $256 \times 256$  and  $32\times$  at  $512 \times 512$ .

## F.2. Complexity Analysis

Table 4 compares the computational cost of Stable Diffusion v1.5 and CoD. Stable Diffusion requires a large captioning model to generate text conditions, whereas CoD relies on a lightweight 177M image encoder and decoder, taking only 8.3 ms to process a  $512 \times 512$  image. The diffusion module in CoD also incurs lower latency and parameter overhead. Pixel-space CoD is slightly slower than latent-space CoD due to the additional decoupled pixel head, but it avoids the expensive VAE decoding, which makes it faster in the few-step regime.

Compared to multi-step diffusion codecs, the one-step pixel-space CoD offers significantly faster inference with a much smaller parameter footprint (see Section B). It enables real-time coding, achieving 25.2 ms per  $512 \times 512$  image. In the future, we hope it can be further accelerated by training a smaller model. Section C demonstrates that CoD can be used as a perceptual supervisory signal, suggesting a promising path toward fast inference: **train a lightweight**

**CoD and distill it into a single step using the large CoD as perceptual supervision.** We leave this direction to future work with the goal of real-time high-resolution diffusion codecs.

## F.3. Additional Evaluation Metrics

Table 6 presents additional performance comparison on the Kodak dataset, with all codecs constrained to approximately 0.004 bpp to ensure a fair evaluation. For the subjective user study, 20 participants rated the reconstruction quality on a scale of 1 (lowest) to 5 (highest), from which Mean Opinion Scores (MOS) were derived. To evaluate semantic preservation, we employed three distinct metrics: (1) CLIP-based visual similarity between original and reconstructed embeddings; (2) text-based similarity between BLIP-2 generated captions of the reconstructions and the ground truth; and (3) a multi-choice Visual Question Answering (VQA) benchmark consisting of 10 GPT-4-designed questions per image. Across all subjective and semantic dimensions, CoD consistently outperforms existing codecs, underscoring its superior generative fidelity.

## F.4. Visual Comparison

In Figure 19, we provide more visual comparison examples. Across a wide bitrate range, CoD-based DiffC presents higher perceptual quality than other codecs.

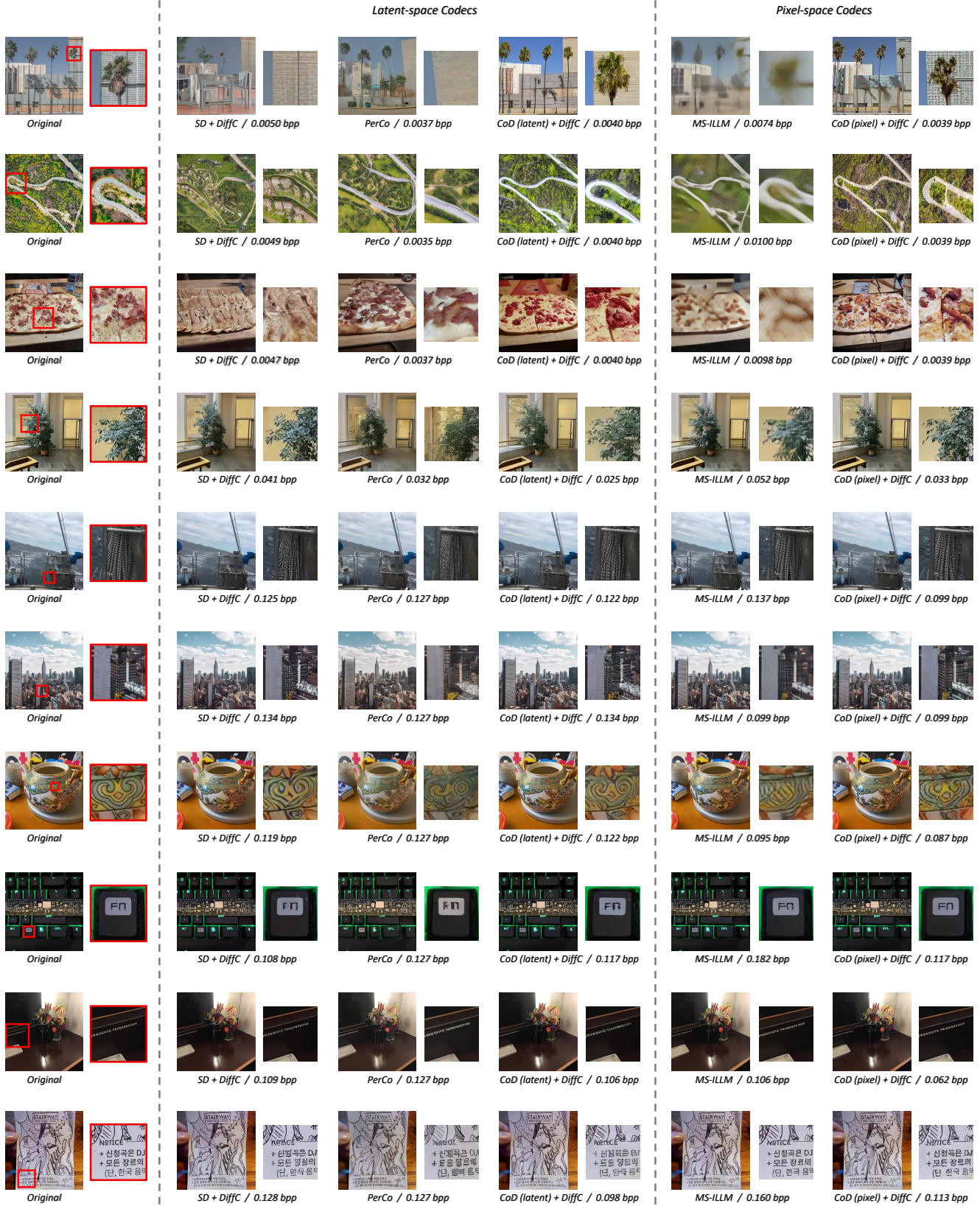


Figure 19. More visualization results on CLIC 2020 test set [44].